A Plane Wave Scattering Dedicated Integral Equation

Benjamin Alzaix, Luc Giraud, Bastiaan Michielsen, Jean-René Poirier

This article has been accepted for publication in a future issue of this journal, but has not been fully edited. Content may change prior to final publication. Citation information: DOI 10.1109/TAP.2019.2948390, IEEE Transactions on Antennas and Propagation

A Plane Wave Scattering Dedicated Integral Equation

B. Alzaix, L. Giraud, B.L. Michielsen, J.-R. Poirier

***Abstract*—We present a variant of a boundary integral equation proposed by M. Herberthson in 2008-2010 for high-frequency plane wave scattering by perfectly conducting obstacles. This integral equation, as some of its predecessors, is entirely dedicated to a single direction of incidence. A significant reduction of the system size can then be obtained by solving for a pseudo-current which is the actual surface current multiplied by the conjugate of the incident wave's phase function. This advantage is mostly lost when multi-incidence problems have to be solved because, in addition to the source terms, also the discretized operator must be recomputed for every new incidence. In this paper, we make an explicit representation of the new operator as the sum of a conventional Electric Field Integral Equation (EFIE) which is independent of the direction of incidence, and an additional operator which takes into account the dependency on the direction of incidence. The latter can be computed very efficiently such that a net performance gain is obtained with respect to the EFIE even for multi-incidence problems.**

***Keywords*—Plane Wave Scattering, Boundary Integral Equations, Model Reduction**

I. Introduction

THE scattering of a plane wave by an impenetrable obstacle can be studied numerically using universal methods like boundary integral equations (Electric Field Integral Equation (EFIE) or Magnetic Field Integral Equation (MFIE)). In this paper, we follow a different strategy in which the computational technique is completely dedicated to the scattering of a given incident plane wave. This has the disadvantage that if the plane wave changes, one needs to reconstruct the model. However, it has the possible advantage that the dedicated model leads to more efficient computations. Such "goal-oriented" approaches to plane wave scattering have been developed before, in particular, with high-frequency scattering problems in mind. The work of Abboud, Nédélec and Zhou (see [1], [2], [3]) published in 1995, is one of the first boundary integral equations where a physical optics approximation is combined with the EFIE. These authors modified the edge element discretization by multiplying the edge elements with the phase function of the incident wave. In a certain way, this makes solving the EFIE to compute a correction with respect to the physical optics approximation. Later work by Darrigrand (see [4]) extended this approach to an alternative integral equation method proposed by B. Després. In these earlier publications, error estimates, based on asymptotic expansions of the solution in the transition to the shadow region, showed that, for convex obstacles, the phase regularization method is warranted to be efficient at high frequencies because the required mesh size decreases in the order of only $\lambda^{1/3}$.

In 2008, Herberthson followed a different track with the same purpose of improving the EFIE performance at high frequencies (see [5], [6], [7]). In his formulation, the incident wave's phase function was incorporated in the kernel distribution of the integral equation, thereby obtaining an integral equation for a pseudo-current defined as the product of the complex conjugate of the incident plane wave's phase function and the physical current distribution. He observed that multiplying both sides of the integral equation with this conjugate phase function yields an exact gradient in the right-hand side. He exploited this further to reduce the conventional EFIE to a system of coupled integral equations for two scalar potentials. Where the previous method was applicable to convex scatterers, Herberthson's version is based on specific topologies (with genus equal to 0) such that the Helmholtz decomposition holds. Roughly speaking, the two points of view lead to increased performance for nearly the same type of geometries.

In this paper, we study a variant of Herberthson's version of the EFIE in order to overcome the restriction to obstacles with special topology. As with the previously mentioned work, the integral equation is specific for plane wave scattering with one chosen direction of incidence. However, representing the operator as an additive perturbation of the conventional one, the perturbation part, which is the only part depending on the phase function of the incident plane wave, can be computed very efficiently.

This splitting allows for the design of a new Galerkin system relaxing the usual constraint of the EFIE with regards to the mesh size and offers the possibility to reduce the number of degrees of freedom required to get an accurate solution of the problem. Considering the conventional equation, and the diffraction of a plane wave with a frequency f_0, a good approximation of the surface current requires the edges of the mesh to have a maximum size h, smaller than $\lambda_0/7$. Working with the pseudo-current and this perturbation splitting, it will be shown that we can effectively work mesh sizes of the order of $\lambda_0/4$.

When considering several directions of incidence, the recomputation of only the perturbation operator leads to a rather low computational overhead.

II. Herberthson's work and a new formulation

In this section, we present Herberthson's modified version for the EFIE. Most of the development can be found in [5], [6], [7]. To set the notations, we assume that an incoming plane wave, with radian frequency ω, illuminates a surface Γ.

B. Alzaix is with Naval GROUP, Ollioules, France

L. Giraud is with INRIA, 200 Avenue de la vieille tour, 33405 Talence, France.

B.L. Michielsen is with Onera/DEMR, Université de Toulouse, 31055 Toulouse France, Bastiaan.Michielsen@Onera.fr

J.-R. Poirier is with LAPLACE, Université de Toulouse, CNRS, Toulouse, France

This article has been accepted for publication in a future issue of this journal, but has not been fully edited. Content may change prior to final publication. Citation information: DOI 10.1109/TAP.2019.2948390, IEEE Transactions on Antennas and Propagation

The plane wave electric field is given in Cartesian coordinates, $r \in \mathbb{R}^3$, by $\boldsymbol{E}^{\text{inc}}(r) = \boldsymbol{e}\psi(r)$ where $\psi(r) = e^{-jk\boldsymbol{u}\cdot\boldsymbol{r}}$ is the phase function of the wave with $\boldsymbol{u}$ the unit vector in the direction of propagation and $k = \frac{\omega}{c}$ the wavenumber (we write $\boldsymbol{r}$ for the vector representation of the coordinates r). The polarization given by $\boldsymbol{e}$ is transverse to the propagation direction, $\boldsymbol{u}\cdot\boldsymbol{e} = 0$. The associated magnetic field is given by $\boldsymbol{H}^{\text{inc}}(r) = Y_0\boldsymbol{u} \times \boldsymbol{e}\psi(r)$ ($Y_0 = \frac{1}{\mu_0 c}$). We let $\boldsymbol{J}$ denote the surface current density. With these notations, the EFIE reads

$$\forall r \in \Gamma \quad \boldsymbol{tr}\left[(\zeta \boldsymbol{I} - \frac{1}{\eta}\nabla\nabla\cdot)\boldsymbol{A}_J\right](r) = \boldsymbol{tr}(\boldsymbol{e}\psi)(r), \qquad (1)$$

where $\zeta = j\omega\mu_0$, $\eta = j\omega\varepsilon_0$ and for a vector-valued function $\boldsymbol{X}$ on $\mathbb{R}^3$, we note $\boldsymbol{tr}(\boldsymbol{X})(r) \equiv (\boldsymbol{n}(r) \times \boldsymbol{X}(r)) \times \boldsymbol{n}(r)$ the tangential component of $\boldsymbol{X}$ in $r \in \Gamma$. The vector potential, $\boldsymbol{A}_J$, is defined by

$$\boldsymbol{A}_J(r) = \int_{r' \in \Gamma} G(r,r')\boldsymbol{J}(r')\mathscr{A}(r').$$

Here $G(r,r')$ is the Green function of the Helmholtz operator defined by

$$G(r,r') = \frac{e^{-jk\|r-r'\|}}{4\pi\|r-r'\|},$$

with $\|r-r'\|$ the Euclidian distance function. Finally, in the surface integral, $\mathscr{A}(r')$ denotes the area element on Γ. In the rest of this paper, we shall leave these area elements implicit in the definition of the integral over Γ and use $\int_\Gamma f \equiv \int_\Gamma f\mathscr{A} = \int_{r\in\Gamma} f(r)\mathscr{A}(r)$.

Now, Herberthson observed that, modulo the phase function ψ, the right-hand side of (1) is the gradient of a scalar function, $\boldsymbol{e} = \nabla(\boldsymbol{e}\cdot r)$. By multiplying both sides of (1) with the complex conjugate of the phase function of the incident plane wave, $\bar{\psi}$, he obtained the following equation,

$$\boldsymbol{tr}\left[\bar{\psi}(\zeta\boldsymbol{I} - \frac{1}{\eta}\nabla\nabla\cdot)\widetilde{A}_{\widehat{\boldsymbol{J}}}\right](r) = -\boldsymbol{e}|_{T_r\Gamma}, \qquad (2)$$

with

$$\widetilde{A}_{\widehat{\boldsymbol{J}}}(r) = \int_{r'\in\Gamma} G(r,r')\psi(r')\widehat{\boldsymbol{J}}(r')\mathscr{A}(r')$$

for a new unknown, $\widehat{\boldsymbol{J}}(r') = \bar{\psi}(r')\boldsymbol{J}(r')$, which we refer to as the pseudo-current.

The second element introduced by Herberthson, is the Helmholtz decomposition. For the special case that Γ is a closed surface diffeomorphic to a sphere, every vector field $\boldsymbol{J}$ on Γ can be decomposed as the sum of a surface gradient, ∇_s, and a co-gradient,

$$\boldsymbol{J} = \nabla_s\Phi + \boldsymbol{n} \times \nabla_s\Psi, \qquad (3)$$

where Φ and Ψ are two scalar functions. In this way, the integral equation (2) can be further transformed into a system of two coupled equations for the scalar potentials Φ and Ψ. In the Galerkin discretization of this system of equations a natural 2×2 block structure appears according to the two potentials and in the right-hand side the terms corresponding to Φ have the value zero.

At this point, our development differs from the one chosen by Herberthson. We remain with the pseudo current vector distribution as the fundamental unknown on an arbitrary surface Γ. The resulting integral equation can, of course, also be seen as a system of coupled equations for the two components of the vector distribution. In that formulation, we can use a special case of the Hodge decomposition which splits off $\ker(\text{div})$. This also gives zero values in the right-hand side corresponding to the testing with $\ker(\text{div})$ functions (with the usual edge finite elements for surface current distributions one can identify a conformal subspace of divergence free functions). Because we have, as yet, not obtained any numerical advantages of using such a decomposition, this aspect will not be further developed here.

III. Algebraic properties

A. Algebraic equivalence between conventional and modified equations

The modified integral equation (2) and the conventional EFIE (1), are actually algebraically equivalent. To show this, we give a description of the two operators $\mathscr{E}$ and $\mathscr{H}$ which define the two equations:

$$\begin{aligned}
\mathscr{E}: \quad & \mathrm{H}_{\text{div}}^{-1/2}(\Gamma) \longrightarrow \mathrm{H}_{\text{curl}}^{-1/2}(\Gamma) \\
& u \longmapsto \boldsymbol{tr}\left[(\zeta\boldsymbol{I} - \frac{1}{\eta}\nabla\nabla\cdot)A_u\right] \\
\mathscr{H}: \quad & \mathrm{H}_{\text{div}}^{-1/2}(\Gamma) \longrightarrow \mathrm{H}_{\text{curl}}^{-1/2}(\Gamma), \\
& v \longmapsto \boldsymbol{tr}\left[\bar{\psi}(\zeta\boldsymbol{I} - \frac{1}{\eta}\nabla\nabla\cdot)\widetilde{A}_v\right],
\end{aligned}$$

where $\mathrm{H}_{\text{div}}^{-1/2}(\Gamma)$ and $\mathrm{H}_{\text{curl}}^{-1/2}(\Gamma)$ are two spaces of distributions on a surface Γ, which can be a piecewise smooth surface such as a triangle mesh. These are, in fact, the spaces of boundary limits and surface restrictions of locally square-integrable vector fields, of which also the curl is locally square integrable. This is precisely the kind of fields which we need for numerical computations with frequency domain electromagnetic fields with locally finite energy.

With these notations, the conventional EFIE reads

$$\mathscr{E}u = -\boldsymbol{tr}(E^{\text{inc}}),$$

whereas the new formulation can be written as:

$$\mathscr{H}v = -\boldsymbol{tr}(\bar{\psi}E^{\text{inc}}). \qquad (4)$$

Then, if we introduce the operator Ψ to denote the multiplication by the Γ-trace of the analytic phase function and Ψ^{-1} its conjugate and inverse, the system (4) can easily be re-written as:

$$\mathscr{H}v = [\Psi^{-1}\circ\mathscr{E}\circ\Psi]v = -\Psi^{-1}\boldsymbol{tr}(E^{\text{inc}}). \qquad (5)$$

Because ψ is a nowhere vanishing C^∞ function, the operator Ψ is a homeomorphism in $\mathrm{H}^s(\Gamma)$ for any s. For the domain of div or the domain of curl, we have the following. For any $u \in \mathrm{H}_{\text{div}}^{-1/2}(\Gamma)$,

$$\text{div}(\psi u) = \nabla\cdot(\psi u) = (\nabla\psi)\cdot u + \psi(\nabla\cdot u)$$

This article has been accepted for publication in a future issue of this journal, but has not been fully edited. Content may change prior to final publication. Citation information: DOI 10.1109/TAP.2019.2948390, IEEE Transactions on Antennas and Propagation

is also in $\mathrm{H}_{\mathrm{div}}^{-1/2}(\Gamma)$, because $(\nabla\psi)\cdot u$ is a sum of $\mathrm{H}^{-1/2}$ coefficients multiplied by C^∞ functions, and $\psi(\nabla\cdot u)$ is the product of a C^∞ function and a $\mathrm{H}^{-1/2}$ function, by the definition of u. Similarly, for any $u\in\mathrm{H}_{\mathrm{curl}}^{-1/2}(\Gamma)$,

$$\mathrm{curl}(\psi u)=\nabla\cdot(\psi u\times n)=(\nabla\psi)\cdot(u\times n)+\psi\nabla\cdot(u\times n),$$

where, again, the first term of the right-hand side is a linear combination of components of $u\times n$ which are in $\mathrm{H}^{-1/2}(\Gamma)$ whereas the second term on the right-hand side is in $\mathrm{H}^{-1/2}(\Gamma)$ by definition of u and the regularity of ψ.

We conclude that the conventional EFIE and the modified EFIE are algebraically equivalent. This means that if the EFIE has a unique solution the modified EFIE also has a unique solution and vice versa. We know that on closed surfaces at discrete frequencies of internal resonance, non-radiating surface currents of undetermined amplitude destroy the uniqueness of the EFIE solution. The algebraic equivalence means that the modified integral EFIE on such closed surfaces has the same non-uniqueness problem at the same set of discrete frequencies. The way these uniqueness problems do actually appear in the discretized integral equation depends on the specific implementation and on the way the resulting linear systems are solved approximately.

IV. Galerkin discretization of the equations

Approximate solutions for the integral equations can be obtained by a Galerkin finite element discretization of the variational formulation.

A. Discretization of the conventional equations

The variational formulation for the conventional EFIE is:

Find $\boldsymbol{J}$ such that for all $\boldsymbol{J'}$ the following equality is satisfied:

$$\zeta a_E(\boldsymbol{J}',\boldsymbol{J})+\frac{1}{\eta}\phi_E(\boldsymbol{J}',\boldsymbol{J})=-\langle\boldsymbol{J}',\boldsymbol{e}\rangle,$$

where $\langle,\rangle$ is the standard distribution evaluation and the bilinear forms in the left-hand side are defined by

$$a_E(\boldsymbol{J}',\boldsymbol{J})=\iint_{(r,r')\in\Gamma^2}G(r,r')\boldsymbol{J}'(r)\cdot\boldsymbol{J}(r')$$

and

$$\phi_E(\boldsymbol{J}',\boldsymbol{J})=\iint_{(r,r')\in\Gamma^2}G(r,r')(\nabla\cdot\boldsymbol{J}')(r)(\nabla\cdot\boldsymbol{J})(r'),$$

respectively. A conformal finite element discretization follows by restricting $\boldsymbol{J}$ and $\boldsymbol{J}'$ to a finite dimensional subspace of $H_{\mathrm{div}}^{-1/2}(\Gamma)$, such as the usual edge element spaces on triangulations.

B. Discretization of the modified equations

The weak formulation of the modified EFIE:

Find $\boldsymbol{J}$, such that for any tangent vector distribution $\boldsymbol{J}'$ on Γ,

$$\zeta a_H(\boldsymbol{J}',\boldsymbol{J})+\frac{1}{\eta}\phi_H(\boldsymbol{J}',\boldsymbol{J})=-\langle\boldsymbol{J}',\boldsymbol{e}\rangle, \tag{6}$$

where

$$a_H(\boldsymbol{J}',\boldsymbol{J})=\iint_{(r,r')\in\Gamma^2}H(r,r')\boldsymbol{J}'(r)\cdot\boldsymbol{J}(r'),$$
$$\phi_H(\boldsymbol{J}',\boldsymbol{J})=\iint_{(r,r')\in\Gamma^2}G(r,r')\nabla\cdot(\bar{\psi}\boldsymbol{J}')(r)\nabla\cdot(\psi\boldsymbol{J})(r')$$

and where we introduced the kernel

$$H:\mathbb{R}^3\times\mathbb{R}^3\ni(r,r')\mapsto H(r,r')=\bar{\psi}(r)G(r,r')\psi(r').$$

C. The modified EFIE as a perturbation of the EFIE

If we describe the operator $\mathscr{H}$ as the sum of the conventional EFIE operator, $\mathscr{E}$, and a perturbation, $\mathscr{K}$, defined by

$$\mathscr{K}=\mathscr{H}-\mathscr{E}, \tag{7}$$

we have isolated the part of $\mathscr{H}$ which depends on the plane wave's direction of incidence. This will appear to be an essential feature of the modified formulations.

For the corresponding bilinear forms $a_K=a_H-a_E$ and $\phi_K=\phi_H-\phi_E$ of the perturbation, we obtain

$$a_K(\boldsymbol{J},\boldsymbol{J}')=\iint_{(r,r')\in\Gamma^2}H_1(r,r')\boldsymbol{J}'(r)\cdot\boldsymbol{J}(r'),$$

with

$$H_1(r,r')=H(r,r')-G(r,r'),$$

and

$$\phi_K(\boldsymbol{J},\boldsymbol{J}')=\iint_{(r,r')\in\Gamma^2}G(r,r')(\nabla\cdot(\bar{\psi}\boldsymbol{J}'))(r)(\nabla\cdot(\psi\boldsymbol{J}))(r')-(\nabla\cdot\boldsymbol{J}')(r)(\nabla\cdot\boldsymbol{J})(r'),$$

which we split into four terms,

$$\begin{aligned}\phi_K(\boldsymbol{J},\boldsymbol{J}')=&\iint_{(r,r')\in\Gamma^2}H_1(r,r')(\nabla\cdot\boldsymbol{J}')(r)(\nabla\cdot\boldsymbol{J})(r')\\&+k^2\iint_{(r,r')\in\Gamma^2}H(r,r')(\boldsymbol{u}\cdot\boldsymbol{J}'(r))(\boldsymbol{u}\cdot\boldsymbol{J}(r'))\\&+jk\iint_{(r,r')\in\Gamma^2}H(r,r')(\boldsymbol{u}\cdot\boldsymbol{J}'(r))(\nabla\cdot\boldsymbol{J})(r')\\&-jk\iint_{(r,r')\in\Gamma^2}H(r,r')(\boldsymbol{\nabla}\cdot\boldsymbol{J}')(r)(\boldsymbol{u}\cdot\boldsymbol{J}(r')).\end{aligned}$$

The integrals involved in a_K and ϕ_K are regular enough to be evaluated numerically since they present no real singularities. This regularity can be shown regarding the kernel's behavior for $r\to r'$. The smoothness of the phase function implies that

This article has been accepted for publication in a future issue of this journal, but has not been fully edited. Content may change prior to final publication. Citation information: DOI 10.1109/TAP.2019.2948390, IEEE Transactions on Antennas and Propagation

the kernel H has the same regularity as the Green function of the Helmholtz operator. This means that the numerical evaluation of the bilinear forms in finite element discretizations can be done with the same techniques as used in the implementations of the conventional EFIE. The kernel H_1 is more regular than the Green function of the Helmholtz operator. Indeed, we have

$$H_1(r,r') \approx -jk\boldsymbol{u}\cdot\boldsymbol{v}(r,r') + O(\|r-r'\|) \quad r \to r',$$

with

$$\boldsymbol{v}(r,r') = \frac{(\boldsymbol{r}-\boldsymbol{r'})}{\|r-r'\|},$$

which is a bounded function (albeit with an undefined value in $r = r'$). This implies that we can numerically compute the internal integrals of a_K and ϕ_K (with Gaussian integration) by applying a specific treatment to the kernel which accounts for this asymptotic behavior when r is close to r'.

In the end, the computation of the perturbation only involves numerical integrations (with Gauss' methods, for example) and a few integrals of singular expressions that are also present in the EFIE and for which efficient implementations have already been found (see, for example, [8, Chapter 2, Section 2.2.1] for a summary of such techniques and further references).

We give in Table I an overview of the floating-point operation count of the computation of H regarding this choice of implementation.

Table I. FLOATING-POINT OPERATION COUNT FOR THE COMPUTATION OF E AND ADDITIONAL COST FOR THE COMPUTATION OF THE MATRIX H.

N_G	Operation count for E		Additional cost for K	
3	$\sim$2.600 F^2	$\sim$1.150 N^2	$\sim$1.482 F^2	$\sim$659 N^2
7	$\sim$13.200 F^2	$\sim$5.850 N^2	$\sim$5.694 F^2	$\sim$2.531 N^2

(F: number of faces, N: number of internal edges, N_G: number of Gauss points considered).

V. REDUCTION OF THE NUMBER OF DEGREES OF FREEDOM

A. Ideas and motivations

In the previous section, we have presented, the formulation of the modified integral equation. However, we did not yet show how to take benefit from its potential advantages. With the modified integral equations, we are solving for a pseudo-current $\widehat{\boldsymbol{J}}$, which is less oscillating than the physical current $\boldsymbol{J}$ on large parts of the surface (see [1]). Fig. 1 illustrates this, with the exact current and pseudo-currents, for the case of plane wave scattering by a perfectly conducting unit sphere.

Even though the pseudo current distribution can be accurately discretized on a rather coarse triangulation, the Galerkin coefficients require integration against a kernel function with possibly great oscillations. On the triangles of a coarse mesh this would require integration rules of much higher order than those usually associated with finite elements. As has already been demonstrated in [1], this makes that the modified EFIE

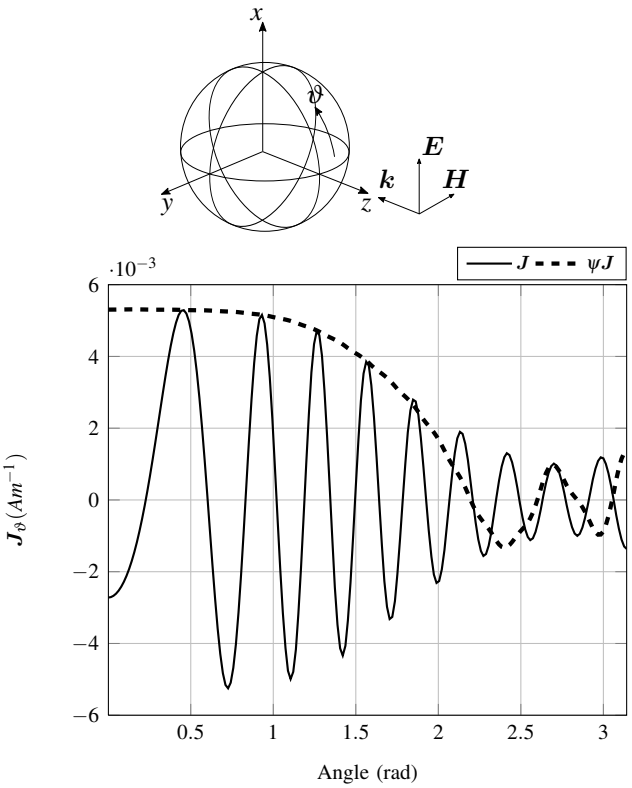

Figure 1. Comparing the oscillations in the physical surface current, $\boldsymbol{J}$, and the pseudo-current, $\overline{\psi}\boldsymbol{J}$, induced on a unit sphere by a plane wave at 1GHz ($\boldsymbol{k} = k\boldsymbol{u}$). The curves represent, in standard spherical coordinates, the real parts of $\boldsymbol{J}_\vartheta$ and $\bar{\psi}\boldsymbol{J}_\vartheta$ as a function of ϑ for $\varphi \equiv 0$.

suffers from the same constraint as the conventional EFIE. In the following paragraphs, we elaborate a technique to deal with this problem.

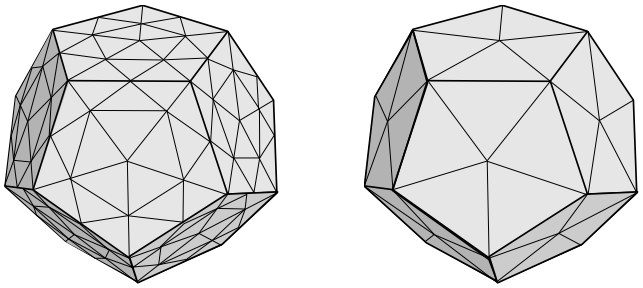

Figure 2. On the left, a fine mesh satisfying the constraints for the EFIE at a given frequency $f = f_0$. On the right, coarse mesh on which we could expect the modified EFIE to give correct results at the same frequency.

B. Macro elements and reduced system

In order to cope with the computational problem observed above, we consider two meshes: a fine mesh satisfying, $h < \lambda_0/7$ (see Fig. 2 on the left), well adapted to work with the

This article has been accepted for publication in a future issue of this journal, but has not been fully edited. Content may change prior to final publication. Citation information: DOI 10.1109/TAP.2019.2948390, IEEE Transactions on Antennas and Propagation

EFIE at given frequency f_0 and allowing proper computations of the Galerkin coefficients, and a coarse mesh, on which we want to discretize the pseudo-currents in the modified equation and which does not necessarily comply with the constraint $h < \lambda_0/7$ (see Fig. 2 on the right).

To avoid ambiguities in the interpretation of the comparisons, we consider the polyhedron of the coarse mesh to be the true geometry. In this way, the finite element spaces in which the modified integral equations are discretized are true subspaces of finite element spaces over a finer mesh. This contrasts to practical applications, where one should use the fine mesh to get a better geometric approximation to the actual boundary surface of the scattering object (For example, by slightly re-distributing the vertices on the actual surface). We shall from now on speak of macro edge elements on macro cells even though the two finite element spaces are more tightly related.

For practical reasons, we start with the coarse mesh and derive the fine mesh from it. For this, we divide each triangle of the coarse mesh into four small triangles by adding a new vertex on the middle of each edge. In this way, starting from a coarse mesh with V_c vertices, E_c edges and F_c faces, we end up with a finer mesh with $V_f = V_c + E_c$ vertices, $E_f = 2E_c + 3F_c$ edges and $F_f = 4F_c$ faces. For a closed surface where $3F = 2E$, we also have $E_f = 4E_c$, such that the dimension of the edge element space on the fine mesh equals four times the dimension of the edge element space on the coarse mesh. The given refinement divides the mesh size by two.

The set of edges of the fine mesh can be partitioned using the macro edges and macro triangles containing them,

$$E_f = \left\{ \bigcup_{\Gamma \in E_c} E_f^\Gamma \right\} \cup \left\{ \bigcup_{T \in F_c} E_f^T \right\},$$

where

$$E_f^\Gamma = \{\Gamma^-, \Gamma^+\}$$

the pair of micro edges arising from the subdivision of the macro edge Γ and

$$E_f^T = \{\gamma_0^T, \gamma_1^T, \gamma_2^T\}.$$

the triplet of micro edges in the interior of macro triangle T.

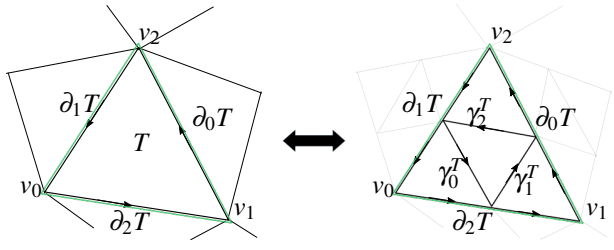

Figure 3. Relation between edge basis functions defined on the coarse mesh and edge basis functions defined on the fine mesh.

The above relations allow us, to construct the Galerkin coefficients of a reduced system over the coarse mesh, using the computations as for the micro elements on the fine mesh, in an update algorithm. Let H_{RED} be the Galerkin matrix over the coarse mesh and H_{FIN} the Galerkin matrix over the fine mesh. As can be inferred from Fig. 3, each macro edge carries a degree of freedom (DoF) which is a linear combination of 8 micro DoF's. We can therefore express the matrix reduction as

$$H_{\text{RED}}^{\Gamma',\Gamma} = \sum_{\gamma' \in e^{\Gamma'}} \sum_{\gamma \in e^\Gamma} c_{\gamma'}^{\Gamma'} c_\gamma^\Gamma H_{\text{FIN}}^{\gamma',\gamma}.$$

using e^Γ for the set of 8 micro edges carrying the micro DoF's contributing to the macro DoF on Γ. The eight coefficients c_γ^Γ have the values $\frac{1}{2}$ or $\pm\frac{1}{4}$ (see the appendix for the details).

Because the kernel of the perturbation operator is more regular than the original kernel of the H operator, we propose an alternative discretization,

$$H_{\text{RED,alt}} = E_{\text{RED}} + K_{\text{COA}},$$

where K_{COA} is the Galerkin matrix of the perturbation operator K, computed directly in the macro element space, whereas E_{RED} is the reduced EFIE Galerkin matrix defined in the same way as H_{RED}. Again, the coefficients of H_{RED} and E_{RED} can be updated "on the fly" from the computation of the coefficients of H_{FIN} and E_{FIN}, respectively, which themselves do not need to be stored (except when we want to use the EFIE on the fine mesh for comparison purposes, of course).

VI. Numerical Results

In this section, we evaluate the modified EFIE with respect to the accuracy of the current distribution on a scattering obstacle and the accuracy of radar cross-section coefficients.

A. Accuracy of the current distribution

In this section, we can compare the results of a conventional EFIE solution on the fine mesh to the solution obtained via the modified EFIE on the coarse mesh. For that purpose, the pseudo-current distribution multiplied by the phase function of the incident wave is represented on the fine mesh. Taking the EFIE result as the reference the relative error is computed via L^2 norms on the fine mesh,

$$\text{Error}(\boldsymbol{J}) = \frac{\|\boldsymbol{J} - \boldsymbol{J}_{FIN}\|_{L^2}}{\|\boldsymbol{J}_{FIN}\|_{L^2}}.$$

1) The unit sphere: The first example concerns a perfectly conducting unit sphere. However, the coarse mesh is again used as the reference geometry and the new vertices of the fine mesh are not displaced to lie on the sphere. In Fig. 4, we show Error($\boldsymbol{J}$) as a function of frequency where 0.2 GHz is the frequency where the mesh size of the coarse mesh equals $\lambda/10$. We observe that H_{RED} and $H_{\text{RED,alt}}$ are very close with a slowly increasing error up to 0.4 GHz ($\lambda/5$). Beyond 0.4 GHz, the error increases more rapidly. The error associated with the regular EFIE based on the coarse mesh is significantly larger and deteriorates rapidly already from 0.05 GHz. From these results, we conclude that $H_{\text{RED,alt}}$ offers the best trade-off between accuracy and computational cost.

This article has been accepted for publication in a future issue of this journal, but has not been fully edited. Content may change prior to final publication. Citation information: DOI 10.1109/TAP.2019.2948390, IEEE Transactions on Antennas and Propagation

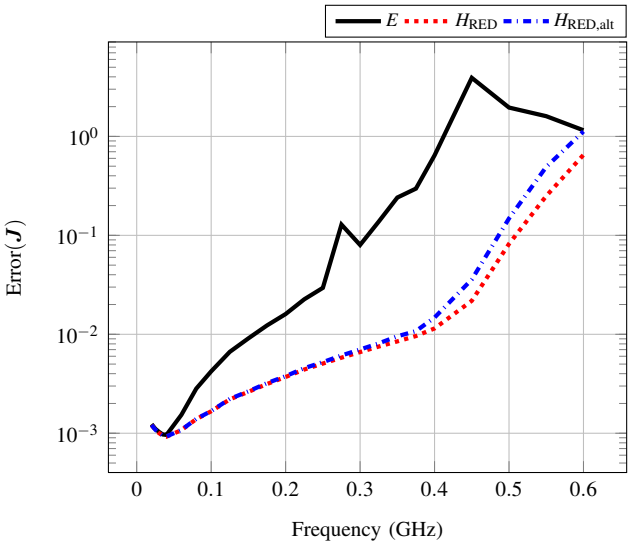

Figure 4. Evolution of the relative error in the surface current on the unit sphere for each of the proposed discretizations (E, H_{RED} and $H_{\text{RED,alt}}$).

2) A flat plate with added surface roughness: We further investigate the accuracy of the various methods on the example of a rectangular plate represented by $(x,y,z) \in (0,L) \times (0,L) \times (-D,0) \subset \mathbb{R}^3$ with $L = 1\ m$, $D = 0.1\ m$. In order to test the performance of the method on a non-convex geometry the flat plate was deformed into a non-convex rough plate using a height profile for the $z = 0$ face, given by

$$h(x,y) = H\left((1-\cos(8\pi x/L))\,(1-\cos(8\pi y/L))\right)$$

where the maximum deformation is $H = 0.1\ m$ (see Fig. 5). The relative errors in the surface current distributions on the

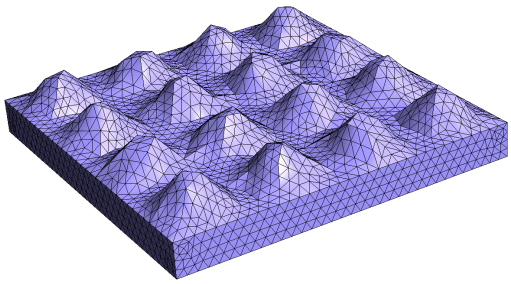

Figure 5. The geometry of the rough plate test case

flat and rough plate obtained with the various techniques are shown in Fig. 6. The observations made for the case of the sphere also apply to these examples. It can be seen that the error jump is significant for the regular EFIE for frequencies larger than 0.5 GHz (corresponding to a mesh size of the order of $\lambda/6$).

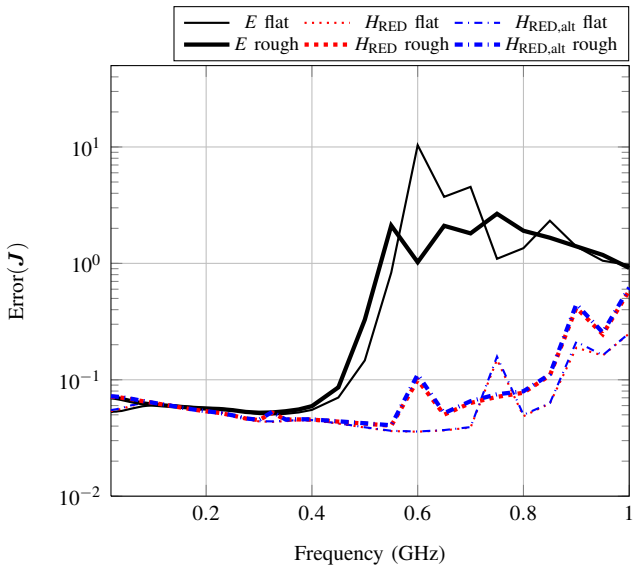

Figure 6. Evolution of the relative error in the surface current distribution as function of the frequency on the flat plate and on the rough plate for each of the proposed discretizations E, H_{RED} and $H_{\text{RED,alt}}$.

The results obtained for the flat plate and the rough plate lead to observations similar to those for the sphere. Nevertheless we can note here that a stronger increase of the error is observed when the mesh size on the rough plate exceeds the value $\lambda/10$ (0.3 GHz). This may be due to the fact that, on this far-from-convex surface, the total variation of the pseudo-current and true surface current are comparable on a large part of the surface.

3) A torus: The original method proposed by Herberthson consisted of representing the pseudo-current distribution as derived from two scalar potentials using a Helmholtz decomposition. This Helmholtz decomposition relies on the non-existence of so-called harmonic surface current distributions, i.e., current distributions with zero Laplacian $\Delta \boldsymbol{J} = 0$. Whether harmonic current distributions exist or not depends on the topology of the surface and the torus is an example where harmonic current distributions do exist indeed. We consider a torus generated by a small circle with radius $r = 0.5\ m$ with its center sweeped along a large circle with radius $R = 1.5\ m$. We computed the surface current distribution induced by a plane wave with propagation direction and electric polarization in the plane of the large circle. The frequency chosen is $0.2\ GHz$, this means that the circumference of the small circle equals $\pi\ m$, i.e. about two wave lengths, and the largest distance between points on the torus is $4\ m$, i.e, a bit more than two and a half wavelengths.

In Fig. 7, the induced current distribution is shown on the surface of a torus. It has been computed on a mesh with 3976 triangles using the conventional EFIE and $H_{\text{RED,alt}}$. The error in the current distribution computed with the modified EFIE (relative to the one obtained with the conventional EFIE) is of

This article has been accepted for publication in a future issue of this journal, but has not been fully edited. Content may change prior to final publication. Citation information: DOI 10.1109/TAP.2019.2948390, IEEE Transactions on Antennas and Propagation

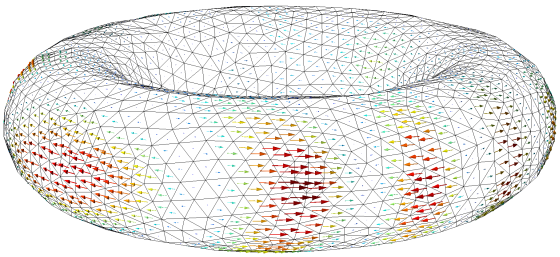

Figure 7. Current distribution on a torus induced by a plane wave at frequency 0.2 GHz

the same order as observed with the rough plate. Again, this is explained by the fact that non-convexity implies multiple scattering between opposite faces, which locally diminishes the correspondence between the current's phase and the phase of the incident wave.

B. Accuracy of bi-static Radar Cross Section coefficients

We further investigate the accuracy of results obtained with the modified EFIE, but this time by looking at bi-static Radar Cross Section computation, which amounts to evaluating the current distributions on plane waves. Note that such bi-static RCS computations are very cheap compared to the computation of the current distribution and we use the same computation. For the perfectly conducting unit sphere, we compare with the analytic solution computed with the Mie series. For the flat plate and the rough plate example, we will use the solution computed with the regular EFIE on the fine mesh as the reference. Because, it appeared as the most promising alternative in the previous section, we only report on experiments with the $H_{\mathrm{RED,alt}}$ version.

1) The unit sphere: Fig. 8 and 9 show a bi-static RCS coefficient computed, for various mesh sizes, with the EFIE and the modified EFIE, respectively. As we are no longer comparing different versions of the modified EFIE, we now place the vertices of the fine meshes on the sphere, which is what one would do in applications of the method.

In Fig. 8, it can be observed that a fairly accurate solution is obtained with the EFIE for a mesh size of $\lambda/7$. This is in good agreement with the classical rule of thumb $\lambda/10$. Similarly, in Fig. 9, we can see that a comparable solution can be obtained with the modified EFIE already for mesh sizes $\lambda/3$ or $\lambda/4$. These experiments illustrate that the new method allows us to relax the mesh size constraint while preserving the same level of accuracy.

2) A flat plate with added surface roughness: For the RCS of a plate with surface roughness, we come to the same conclusions as for the example of the sphere. We consider a plane wave, at 1 GHz, normally incident on the rough face of the plate and with electric polarization parallel to one of the edges of the plate. This time, we compare the bi-static RCS to results computed with the commercial code FEKO on a mesh

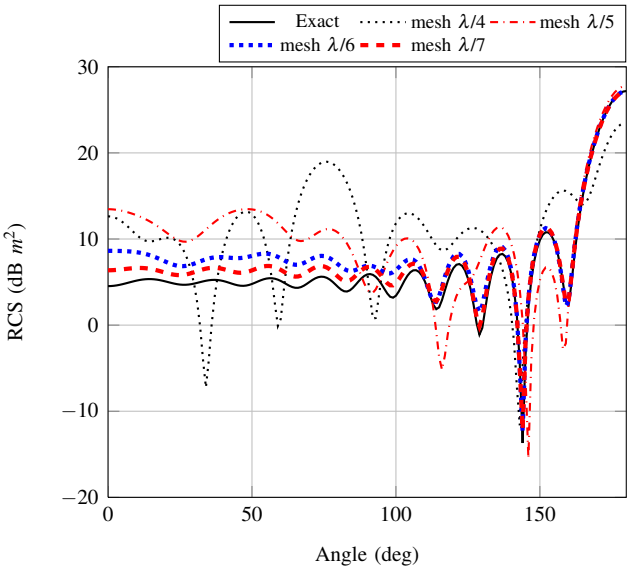

Figure 8. Representation of the bi-static RCS of the unit sphere obtained from the various meshes with the EFIE at $f = 0.6\,GHz$.

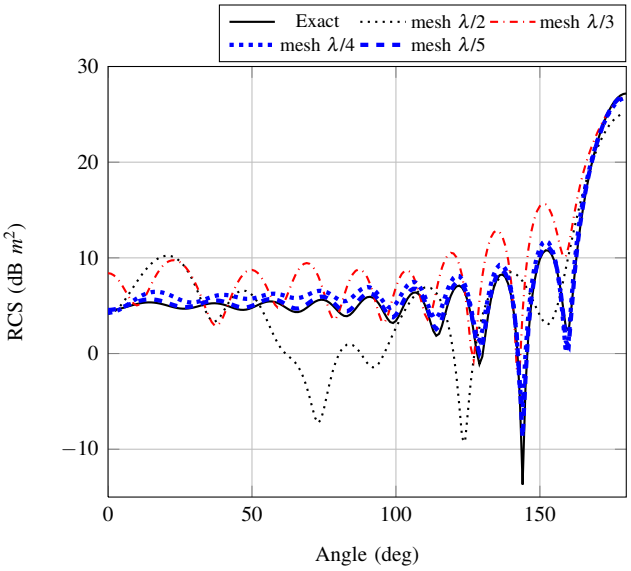

Figure 9. Representation of the bi-static RCS of the unit sphere obtained from the various meshes with the modified EFIE system using $H_{\mathrm{RED,alt}}$ at $f = 0.6\,GHz$.

satisfying the constraint $h < \lambda/10$ on the mesh size. It can be seen that the modified EFIE $H_{\mathrm{RED,alt}}$ obtains the reference result with a rather coarse mesh when the conventional EFIE is significantly different from the actual values. The efficiency of the modified EFIE is even more pronounced for oblique incidence (see Fig. 11) 45° off the normal in the same plane of incidence. (We use these results also as a validation of our implementation of the conventional EFIE.)

This article has been accepted for publication in a future issue of this journal, but has not been fully edited. Content may change prior to final publication. Citation information: DOI 10.1109/TAP.2019.2948390, IEEE Transactions on Antennas and Propagation

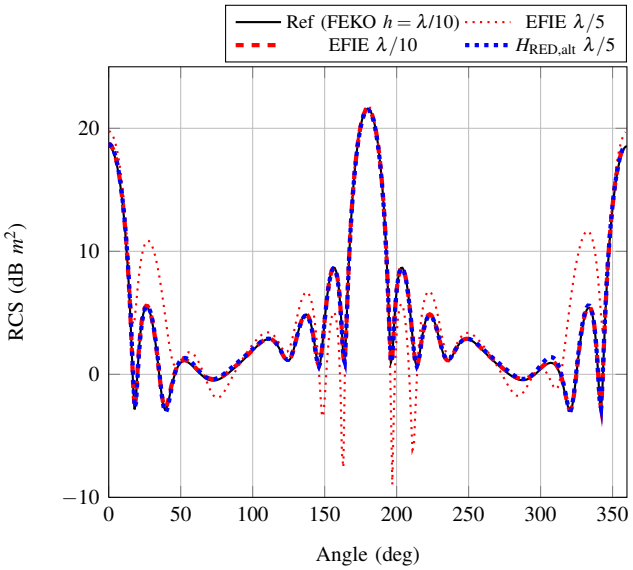

Figure 10. Comparison of the bi-static RCS for normal incidence on the rough plate at $f = 1\,GHz$ obtained with FEKO and with $H_{\text{RED,alt}}$. The FEKO and EFIE at $\lambda/10$ curves coïncide.

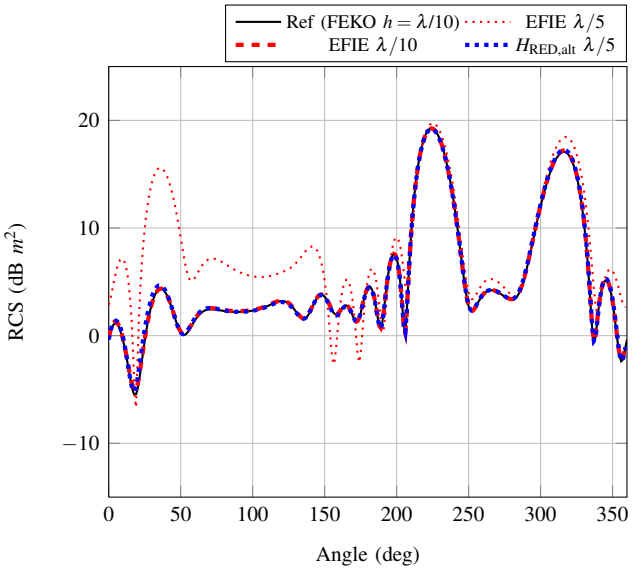

Figure 11. Comparison of the bi-static RCS for oblique incidence on the rough plate at $f = 1\,GHz$ obtained with FEKO and with $H_{\text{RED,alt}}$.

3) A torus: For the non-convex geometry of a torus, we compute the bi-static RCS graphs in the plane of incidence containing the center of the torus and orthogonal to the electric polarization lying in the plane of the large circle of the torus. Even though the current distribution obtained with the modified EFIE can have relative errors up to 10 percent with respect to the exact current distribution, the bi-static-RCS results are practically indistinguishable (see Fig. 12). This means that even for this type of non-convex objects an important reduction

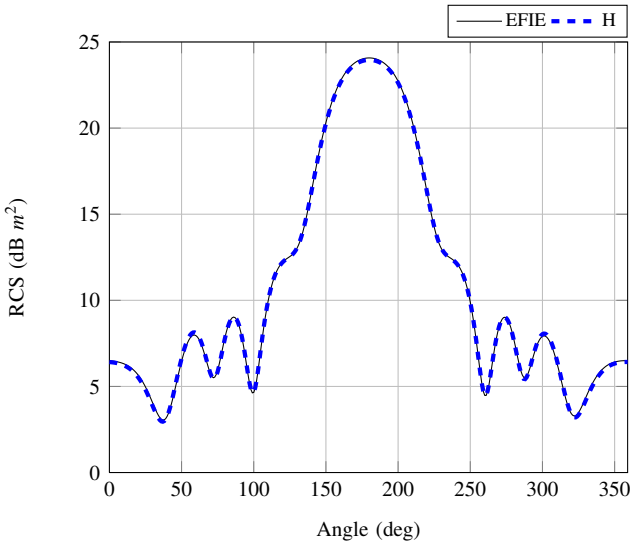

Figure 12. Bi-static RCS result of a torus in the plane of incidence computed with the conventional EFIE on a $\lambda/10$ mesh and the modified EFIE on a $\lambda/5$ mesh at frequency 0.2 GHz

of the number of unknowns can be obtained without loosing accuracy if the quantities of interest are scattering coefficients.

C. Performance comparison

In this section, we compare the performances of the modified EFIE and the conventional EFIE with respect to memory and CPU time requirements, for a given desired accuracy. The example problems presented in the preceding sections are relatively small and have been solved with direct methods (numpy.linalg.solve). In order to investigate the advantages for larger problems, requiring iterative solution methods, we also solved the EFIE and modified EFIE problems with a GMRES (Generalized Minimal RESidual) iterative solution algorithm. We included the GMRES stopping criterion, ε_{GMRES}, as a parameter in our tests.

The modified EFIE has clear advantages from a memory point of view because, as we have seen, it requires about 4 times less degrees of freedom than the conventional EFIE for a given accuracy. With a given amount of available memory, this allows one to handle objects of larger size relative to the wavelength than is possible with the EFIE. This is illustrated in Fig. 13, where one observes that for a given available memory, the modified EFIE can reach better precision than the conventional EFIE.

In Fig. 14, we show, for the EFIE and the modified EFIE, at a given required accuracy, the total execution time, i.e., the sum of the time needed to construct the linear system and the time to obtain the solution.

In both Fig. 13 and Fig. 14, we observe that the two methods have roughly the same performance. The total solution time with the modified EFIE depends less on the stopping criterion, ε_{GMRES}, than with the conventional EFIE. This is because the

This article has been accepted for publication in a future issue of this journal, but has not been fully edited. Content may change prior to final publication. Citation information: DOI 10.1109/TAP.2019.2948390, IEEE Transactions on Antennas and Propagation

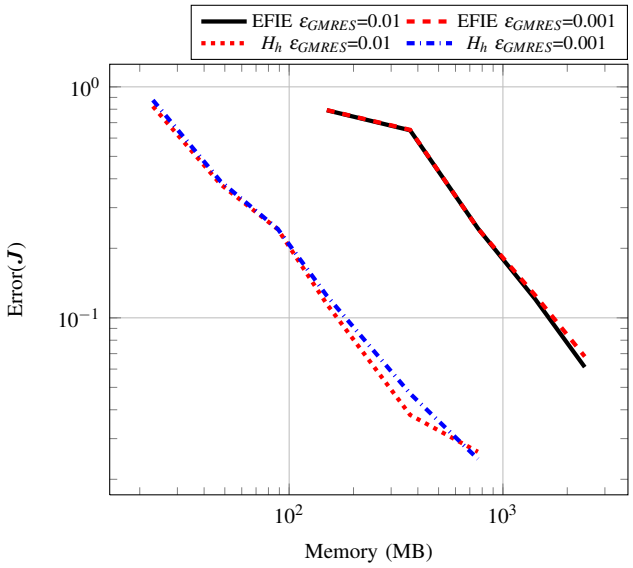

Figure 13. Relative error in the computed current distribution as a function of the available memory for several values of ε_{GMRES}. All methods show the same tendency, but the modified EFIE allows to obtain better precision in when limited memory is available.

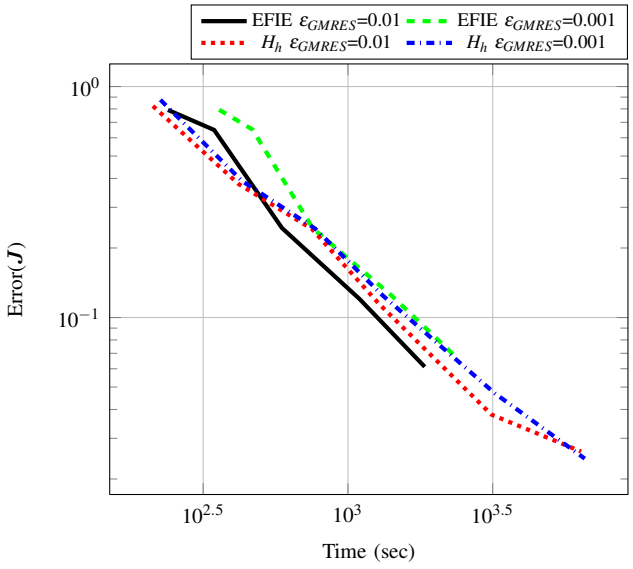

Figure 14. Relative error in the computed current distribution as a function of the total computation time for several values of ε_{GMRES}. Given the current implementation, if computation time as allowed to increase the relative error goes down in roughly the same way with all methods tested.

system construction time in the examples dominates the total execution time. The fact that for better accuracies the EFIE results are absent is due to the fact that the EFIE memory requirements exceeded the available memory on the computer used.

In the context of multi-incidence problems the advantages of the modified EFIE depend on the cost of recomputation of the K_{COA} matrix for each new incidence compared to the time spent in each iteration with the conventional operator. Because computation times of iterative solution methods strongly depend on the chosen operator representation (Fast Multipole Method (FMM), Adaptive Cross Approximation (ACA), hierarchical (HCA), ...), we cannot make universal statements here. We just want to note that for the GMRES methods iterating with the full Galerkin matrices, as used in the tests which led to Figs. 13 and 14, the additional cost of computing K_{COA} for a new incidence is largely compensated by the gain in computation time spent in the iterations with much smaller matrices. The fact that the dimension of the problem is reduced by a factor 4 is clearly the dominant feature.

VII. Conclusion and Perspectives

We have presented a modified version of the electric field integral dedicated to plane wave scattering problems. This formulation allows one to escape from certain limitations of the conventional EFIE in terms of discretization dimensions at high frequencies. The results of various comparisons shown in this paper lead to the conclusion that the new formulation is clearly advantageous. This is, above all, due to the fact that, for comparable accuracy at identical problems, roughly 4 times less unknowns are needed than with the conventional EFIE. According to previous work, this ratio will be more and more in favor of the modified EFIE when the frequency increases.

Although the numerical results obtained are promising, a more exhaustive study deserves to be undertaken. In particular, comparisons should be performed with numerical implementations accommodating compression techniques such as FMM or hierarchical matrix calculations. It can also be noticed that the new integral equation has an advantage in terms of system solving time, when using a GMRES iterative method. This lets us expect to obtain advantageous performance for multiple right-hand sides (multiple incidence directions) where the gain in solving time outweighs the additional cost needed to construct the incidence direction dependent perturbation matrix ($K = H - E$) which can be done on a rather coarse mesh.

However, these perspectives need to be confirmed by a numerical study for objects of larger size. This work will include the elaboration of acceleration techniques like FMM, ACA or HCA with H-Matrix calculations. The HCA techniques (see [9], [10]) will be our most favorable candidates because they allow us to work directly on the optimization of the numerical integration rules.

Appendix
Details of the Model Reduction

In this appendix, we present the details of the reduction of the edge element Galerkin matrix on the fine mesh to one on the coarse mesh. Fixing the ordering of the added edges makes it easier to handle the relation between the edge element spaces on the coarse and the fine mesh. Here, we choose to order the edges added in the interior of a triangle of the coarse mesh according to the positive orientation of this triangle (see Fig. 3). Each macro edge Γ, corresponds to an ordered pair of

This article has been accepted for publication in a future issue of this journal, but has not been fully edited. Content may change prior to final publication. Citation information: DOI 10.1109/TAP.2019.2948390, IEEE Transactions on Antennas and Propagation

two micro edges $\Gamma = (\Gamma_-, \Gamma_+)$ oriented consistently with the orientation of Γ.

For the degree of freedom (DoF) associated with the macro edge $\partial_p T$, we have two micro DoF's associated with the two micro edges contained by the macro edge, and three micro-DoF's on the micro-edges, γ_p^T, $p \in \{0,1,2\}$, internal to each of the two macro-triangles, $T = \partial^{*+}\Gamma$ and $T = \partial^{*-}\Gamma$, adjacent to the macro-edge Γ (only one of these macro-triangles, $\partial^{*+}\Gamma$, is shown in Fig. 3).

We write

$$e^\Gamma = E_f^\Gamma \oplus E_f^{\partial^{*-}\Gamma} \oplus E_f^{\partial^{*+}\Gamma}$$

for the ordered octuple of micro-edges associated with Γ.

Let basis functions of an edge finite element space be labeled by the edge fixing the degree of freedom. We write J^Γ for a macro basis function associated with a macro edge Γ and j^γ for a micro basis function associated with a micro edge γ.

The macro basis function, J^Γ, can be written generically as a sum

$$J^\Gamma = \sum_{\gamma \in e^\Gamma} c_\gamma^\Gamma j^\gamma.$$

The coefficients are defined as follows:

$$c_\gamma^\Gamma = \begin{cases} \frac{1}{2} & \text{if } \gamma \in \{\Gamma_-, \Gamma_+\} \\ \mp\frac{1}{4} & \text{if } \gamma = \gamma_p^T \text{ and } \Gamma = \pm\partial_p T \\ \pm\frac{1}{4} & \text{if } \gamma = \gamma_p^T \text{ and } \Gamma = \pm\partial_q T \text{ with } p \neq q. \end{cases}$$

The value $\frac{1}{2}$, is obtained because of the subdivision of any macro edge in two equal halves. The 4 sub triangles of a triangle T, have equal area, $\frac{|T|}{4}$, because they are spanned by edges which are parallel to and exactly half the size of two macro edges. As the edge elements have constant divergence, each flow entering a micro triangle should leave it with a flow $\frac{1}{4}$ smaller. The specific distribution of signs follows from the choice of orientation of the micro edges and the orientation of the macro edge relative to the positive orientation of the macro triangle. These must be taken as they come with the coarse mesh (we cannot suppose any specific rule here).

It should be clear that all the mappings and associated data structures can be defined while constructing the refinement by sweeping through the coarse mesh for which the boundary operator and all DoF administration is already available (See [11] for more details and [12] for alternative methods).

REFERENCES

[1] Bin Zhou. *Méthode des équations intégrales pour la résolution des problèmes de diffraction à hautes fréquences*. PhD thesis, Paris 11, 1995.

[2] T. Abboud, J.-C. Nédélec and B. Zhou. Méthodes des équations intégrales pour les hautes fréquences. *C. R. Acad. Sci. Paris*, (318):165–170, 1994.

[3] T. Abboud, J.-C. Nédélec and B. Zhou. Improvement of the integral equation method for high frequency problems. *Third International Conference on Mathematical and Numerical Aspects of Wave Propagation*, pages 178–187, 1995.

[4] Eric Darrigrand. *Couplage Méthodes Multipôles - Discrétisation Microlocale pour les Equations Intégrales de l'Electromagnetisme*. PhD Thesis, Université Sciences et Technologies - Bordeaux I, Sep 2002.

[5] M. Herberthson. Validation of the Potential Method ; Comparing measurements of a dihedral with calculations . *Scientific Computing in Electrical Engineering conference, Zurich*, 2012.

[6] Magnus Herberthson. EM Scattering Calculations Using Potentials. *Scientific Computing in Electrical Engineering SCEE 2008*, pages 375–382, 2010.

[7] Magnus Herberthson. Application of the Potential Method to the Combined Field Integral Equation. *Scientific Computing in Electrical Engineering SCEE 2010 (Abstract book)*, pages 103–104, 2012.

[8] Eric Darve. *Méthodes multipôles rapides : résolution des équations de Maxwell par formulations intégrales*. PhD thesis, Paris 6, 1999.

[9] Steffen Börm and Lars Grasedyck. Hybrid cross approximation of integral operators. *Numerische Mathematik*, 101:221–249, 2005.

[10] P. Daquin, R. Perrussel, and J.-R. Poirier. Hybrid Cross Approximation for the Electric Field Integral Equation. *Progress In Electromagnetics Research M*, 75:79–90, 2018.

[11] Benjamin Alzaix. *Mathematical and numerical analysis of the Herberthson integral equation dedicated to electromagnetic plane wave scattering*. PhD thesis, Université de Bordeaux, Avril 2017.

[12] F.P. Andriulli. Loop-Star and Loop-Tree Decompositions: Analysis and Efficient Algorithms. *IEEE Transactions on Antennas and Propagation*, 60(5):2347–2356, May 2012.

Benjamin Alzaix received the Engineering degree from INSA Toulouse, France, in 2013. The present publication reports on part of his PhD work done at Onera in collaboration with ENSEEIHT and INRIA. He obtained his PhD in 2017 and since then works at Naval Group in Toulon, France.

Luc Giraud holds a doctorate in computer science from the Institut National Polytechnique de Toulouse. He joined CERFACS successively as a researcher, ENSEEIHT as a full professor in applied mathematics and finally INRIA as senior researcher where he is currently leading a team addressing numerical techniques for large computing platforms.

Bastiaan Michielsen received the Engineering degree from Delft University of Technology in 1980. After military service at TNO's microwave laboratory he worked from 1982 to 1991, at PHILIPS Research Laboratories in Eindhoven, The Netherlands, and in Redhill, United Kingdom. Since 1991 he works at Onera in France. His main research interests are in electromagnetic theory and boundary integral equations, including the analysis of geometrical uncertainties.

Jean-René Poirier received the Engineer diploma from INSA, Toulouse, France in 1996. He was a Ph.D. student at Onera from 1997 to 2000 and received the Ph.D. degree in applied mathematics from INSA in december 2000. From 2001 to 2003, he joined the Analysis and Scientifc Computing group from EPFL, Switzerland. He is currently working as an associate professor at INPT- ENSEEIHT, Toulouse, and joined the LAPLACE laboratory, in January 2009. His current research interests focus on computational electromagnetics and include rough surface scattering, boundary impedance condition and fast solvers for boundary element method.